



# LUND UNIVERSITY

## Exploiting antenna correlation in measured massive MIMO channels

Flordelis, Jose; Hu, Sha; Rusek, Fredrik; Edfors, Ove; Dahman, Ghassan; Gao, Xiang; Tufvesson, Fredrik

*Published in:*

2016 IEEE 27th Annual International Symposium on Personal, Indoor, and Mobile Radio Communications, PIMRC 2016

*DOI:*

[10.1109/PIMRC.2016.7794664](https://doi.org/10.1109/PIMRC.2016.7794664)

2016

*Document Version:*

Peer reviewed version (aka post-print)

[Link to publication](#)

*Citation for published version (APA):*

Flordelis, J., Hu, S., Rusek, F., Edfors, O., Dahman, G., Gao, X., & Tufvesson, F. (2016). Exploiting antenna correlation in measured massive MIMO channels. In *2016 IEEE 27th Annual International Symposium on Personal, Indoor, and Mobile Radio Communications, PIMRC 2016* Article 7794664 IEEE - Institute of Electrical and Electronics Engineers Inc.. <https://doi.org/10.1109/PIMRC.2016.7794664>

*Total number of authors:*

7

### General rights

Unless other specific re-use rights are stated the following general rights apply:

Copyright and moral rights for the publications made accessible in the public portal are retained by the authors and/or other copyright owners and it is a condition of accessing publications that users recognise and abide by the legal requirements associated with these rights.

- Users may download and print one copy of any publication from the public portal for the purpose of private study or research.
- You may not further distribute the material or use it for any profit-making activity or commercial gain
- You may freely distribute the URL identifying the publication in the public portal

Read more about Creative commons licenses: <https://creativecommons.org/licenses/>

### Take down policy

If you believe that this document breaches copyright please contact us providing details, and we will remove access to the work immediately and investigate your claim.

LUND UNIVERSITY

PO Box 117  
221 00 Lund  
+46 46-222 00 00

# Exploiting Antenna Correlation in Measured Massive MIMO Channels

Jose Flordelis, Sha Hu, Fredrik Rusek, Ove Edfors, Ghassan Dahman, Xiang Gao and Fredrik Tufvesson

Dept. of Electrical and Information Technology, Lund University, Lund, Sweden

Email: *firstname.lastname@eit.lth.se*

**Abstract**—We investigate antenna correlation of an  $M$ -antenna massive multiple-input multiple-output (MIMO) setup with the purpose of obtaining a low-rank representation of the instantaneous massive MIMO channel. Low-rank representation bases using short-term and long-term antenna correlation statistics are defined, and their performance is evaluated with data sets obtained from channel measurements in both indoor and outdoor environments at 2.6 GHz. Our results indicate that the short-term bases can capture a larger amount of the channel energy compared to the long-term ones, but they have a limited time-span, one coherence time or less. On the other hand, the long-term bases are stable over time-spans of a few seconds. Hence, they can be obtained relatively easily. We also investigate a rank- $p$  vector-scalar LMMSE channel estimator that exploits antenna correlation. Our results show that the investigated estimator can achieve a performance similar to that of full-rank LMMSE at a  $(2p+1)/M$  times lower cost. The investigated estimator may be used in conjunction with estimators that exploit correlation in the frequency and time domains or, alternatively, in situations in which these estimators cannot be used, e.g., when pilot separation is larger than the channel coherence bandwidth or time.

## I. INTRODUCTION

Massive multiple-input multiple-output (MIMO) is a communication technology that has the potential to enable substantial improvements in spectral and energy efficiency compared to state-of-the-art systems [1], [2]. In a typical massive MIMO system, an  $M$ -antenna base station (BS) communicates with  $K$  single-antenna users, with  $M$  much larger than  $K$ . By exploiting the spatial degrees of freedom arising from the surplus of BS antennas, users can be served simultaneously and independently while making use of simple, linear processing schemes. Because of this, massive MIMO is regarded as an avenue towards future 5G communication systems [3], [4].

It is well-known that wireless channels, when incorporating the effects of the transmit and receive antennas, are usually correlated at both link ends. In contrast to conventional multiple-user multiple-antenna systems, in which antenna correlation has normally an adverse effect, there are a few cases in massive MIMO where it can be advantageous. For example, the authors of [5], [6] propose a two-stage precoding scheme termed joint spatial division and multiplexing (JSDM) which, by judiciously exploiting the structure of the correlation of the channel vectors, achieves significant savings in uplink feedback, thus potentially enabling frequency division duplex (FDD) massive MIMO. In the same vein, [7]–[9] suggest feedback compression algorithms which rely on low-rank approximations to the covariance matrix of the channel vectors.

These approximations are feasible provided that antennas at the BS are highly correlated.

However, although techniques that exploit the structure of the spatial correlation of the massive MIMO channel have recently received a fair amount of attention [5]–[9], little [10] seems to have been reported on *measurements* of such correlations. This paper has two main contributions. First, we investigate two types of reduced-rank bases for representing spatially correlated channel vectors, short-term and long-term, and report on their efficiency and stability properties. Second, as an application of the above, we investigate a rank- $p$  ( $p \leq M$ ) vector-scalar linear minimum mean-squared error (LMMSE) channel estimator that exploits the spatial correlation of the massive MIMO channel. The investigated estimator has  $(2p+1)/M$  times lower complexity, yet performs similarly to the full-rank, optimal LMMSE estimator. The investigated estimator is especially useful in situations in which correlation in the frequency-time domain cannot be readily exploited, e.g., when pilot separation is larger than the channel coherence bandwidth or time. We would also like to point out that the investigated algorithm is not restricted in any way to processing signals in the spatial domain; on the contrary, it can be applied to any general vector estimation problem.

The rest of the paper is organized as follows. In Sec. II, the system model is presented. After that, the channel measurement campaigns are introduced in Sec. III. In Sec. IV, the theory of optimal representation basis is shortly reviewed, and then applied to the measurement data. Next, channel estimators that exploit antenna correlation in massive MIMO systems are discussed in Sec. V. Finally, Sec. VI concludes the paper.

## II. SYSTEM MODEL

In this work, as we do not consider the massive MIMO precoding or detection steps, all signal processing is carried out independently for each user. Because of this, the original multi-user problem can be reduced to the single-user case. We thus consider a single-antenna user communicating with an  $M$ -antenna BS,  $M \gg 1$ . Further, we assume that orthogonal frequency division multiplexing (OFDM) [11] is used. As such, the channel is decomposed into  $L$  parallel noninteracting subcarriers, each of them experiencing frequency-flat fading. Let  $\mathbf{h}(n, \ell) \in \mathbb{C}^M$  denote the channel vector from the user to the BS at symbol  $n = 1, \dots, N$  and subcarrier  $\ell = 1, \dots, L$ . Then, the baseband complex representation of the signal received at the BS can be written as

$$\mathbf{y}(n, \ell) = \mathbf{h}(n, \ell) s(n, \ell) + \mathbf{n}(n, \ell), \quad (1)$$

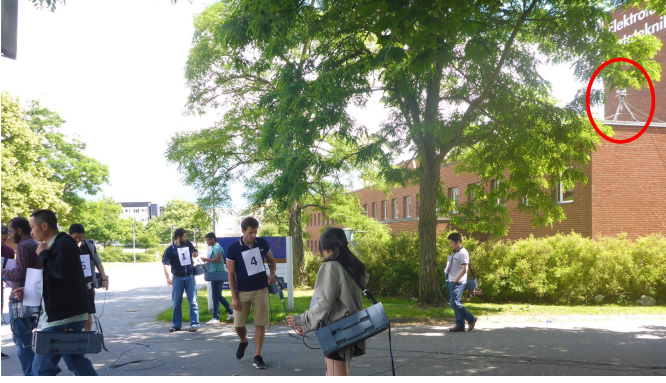


Fig. 1.  $K = 9$  users in an outdoor environment. Note the BS antenna encircled in red.

where  $s(n, \ell) \in \mathbb{C}$  is the transmit signal, which fulfills  $\mathbb{E}[s(n, \ell)s^*(n, \ell)] = P$ , and  $\mathbf{n} \in \mathbb{C}^M$  is the vector of additive receiver noise distributed according to  $\mathcal{CN}(0, N_0\mathbf{I})$ .

In some parts of our discussion, the model without additive noise

$$\mathbf{y}(n, \ell) = \mathbf{h}(n, \ell) s(n, \ell) \quad (2)$$

will be used instead. When this is the case, it will be clearly indicated.

### III. MEASUREMENT DESCRIPTION

To study the correlation properties of antenna elements in real propagation environments, we select data sets from two massive MIMO channel measurement campaigns corresponding to one outdoor and one indoor scenarios. In both measured scenarios, 9 single-antenna users located close to each other communicate with a BS mostly in LOS propagation conditions. At the BS, a switched antenna array with 64 dual-polarized patches (i.e.,  $M = 128$  antenna ports) arranged in cylindrical geometry is used. Outdoor measurements took place at the campus of the faculty of engineering LTH of Lund University, Lund, Sweden (55.711510 N, 13.210405 E), in a suburban environment. In this setup, users moved randomly at speeds at most 0.5 m/s while being confined to a 5 meter diameter circle. The BS was located on a nearby rooftop at a height of 9 m (see Fig. 1). A map of the environment is available in [12], which reports on a related massive MIMO campaign.

Indoor measurements took place in lecture theater E:A, which is part of the E-building at LTH. In this case, although the positions of the users were static, UE antennas moved in random circular trajectories in front of the torso of the users (see Fig. 2). UE antennas can be thought of as revolving around a 0.5 meter diameter circumference at an angular velocity  $\omega \approx \pi$  rad/s. The outdoor and indoor scenarios selected are representative of propagation conditions arising in outdoor live concerts and sport events, and in indoor concert halls and conference venues, respectively.

Measurement data were recorded using the RUSK LUND MIMO channel sounder [13]. The principal configuration parameters of the RUSK LUND channel sounder are shown in Tab. I. Here is an interesting observation that will be useful later when we discuss the stability of the representation bases. We observe that, in both the indoor and the outdoor



Fig. 2.  $K = 9$  users in a lecture theater.

TABLE I. RUSK LUND PRINCIPAL CONFIGURATION PARAMETERS.

Parameter	Value (indoors/outdoors)
Carrier frequency ( $f_c$ )	2.6 GHz
Measurement bandwidth	40 MHz
Number of Tx-Rx pairs ( $N_{\text{ch}}$ )	$9 \times 128$
Number of subcarriers ( $L$ )	129 / 257
Maximum measurable delay ( $\tau_{\text{max}}$ )	$3.2 / 6.4 \mu\text{s}$
Snapshot duration	$2 \times N_{\text{ch}} \times \tau_{\text{max}}$
Snapshot sampling rate	17 Hz
Number of snapshots ( $N$ )	300
Nominal output power	27 dBm

setups, UE antennas are confined to small regions of the space. Because of this, we expect that most of the energy between each UE antenna and the BS propagates through a limited set of independent paths. As the UE antenna travels within this finite region, the different paths are revealed. Hence, after a suitably long observation time, we expect that a stable long-term representation basis can be obtained. One can expect to have one such long-term basis per geographic location. Whether or not short-term bases stay constant longer than the channel coherence time will depend, for each geographic location, on the local stationarity properties of the channel.

We should also mention that, even though the number of independent propagation paths might be limited, the instantaneous channel is usually not “static”. Indeed, the radio channel between each measured transmit-receive antenna pair changes quickly. If we consider the channel as being approximately constant for UE antenna displacements less than  $\lambda_c/4$ , its coherence time can be estimated as

$$T_{\text{coh}} = 0.25 \times (\lambda_c/v), \quad (3)$$

where  $v$  is the speed of the UE antenna, and  $\lambda_c$  is the wavelength at the carrier frequency. In the outdoor setup,  $v = 0.5$  m/s gives  $T_{\text{coh}} \approx 58$  ms. For the measured indoor scenario, we can compute  $v = 0.25 \times \omega = \pi/4$  m/s, which gives  $T_{\text{coh}} \approx 37$  ms. Hence, the coherence time and the time between snapshots ( $1/17 \approx 59$  ms) have the same order of magnitude. This will somewhat limit our ability to study the temporal stability of the short-term bases.

### IV. REPRESENTATION BASES

In this section, we first define the notion of short-term and long-term representation bases. Then, we introduce the concept of normalized captured channel energy as a figure of merit, and apply it to the channel measurement data.

### A. Optimal Short-Term and Long-Term Representation Bases

Consider the orthonormal basis  $\mathbf{B}$  of dimension  $p$ . Then, we can write

$$\mathbf{h}(n, \ell) = \mathbf{f}(n, \ell) + \mathbf{e}(n, \ell), \quad (4)$$

where  $\mathbf{f}(n, \ell) = \mathbf{B}\mathbf{B}^H\mathbf{h}(n, \ell)$  is the representation of  $\mathbf{h}(n, \ell)$  in the basis  $\mathbf{B}$ , and  $\mathbf{e}(n, \ell) = (\mathbf{I} - \mathbf{B}\mathbf{B}^H)\mathbf{h}(n, \ell)$  is the representation error. We seek a basis  $\mathbf{B}$  that minimizes the energy of the representation error across all subcarriers within a certain observation time.

First, consider the matrix

$$\mathbf{A}(n) = [\mathbf{h}(n, 1) \cdots \mathbf{h}(n, L)], \quad (5)$$

formed by collecting the channel vectors at OFDM symbol  $n$  and subcarriers  $\ell = 1, \dots, L$ , and its singular value decomposition (SVD)

$$\mathbf{A}(n) = \mathbf{U}(n)\mathbf{\Sigma}(n)\mathbf{V}(n)^H, \quad (6)$$

where  $\mathbf{U}(n) = [\mathbf{u}_1(n) \cdots \mathbf{u}_M(n)] \in \mathbb{C}^{M \times M}$  and  $\mathbf{V}(n) = [\mathbf{v}_1(n) \cdots \mathbf{v}_L(n)] \in \mathbb{C}^{L \times L}$  are unitary matrices, and  $\mathbf{\Sigma}(n) \in \mathbb{R}^{M \times L}$  is a diagonal matrix  $\sigma_1(n) \geq \dots \geq \sigma_q(n) \geq 0$ , where  $q = \min(M, L)$ . Then,

$$\mathbf{B}_{\text{SVD}}(n) = [\mathbf{u}_1(n) \cdots \mathbf{u}_p(n)] \quad (7)$$

is an optimal  $p$ -dimensional representation basis of the column space of  $\mathbf{A}(n)$ . Since  $\mathbf{B}_{\text{SVD}}(n)$  depends on a single OFDM symbol, it can be regarded as a *short term* or *instantaneous* representation basis. Depending on the local properties of the channel, the optimal basis  $\mathbf{B}_{\text{SVD}}(n)$  might change quickly. In such cases, to preserve optimality,  $\mathbf{B}_{\text{SVD}}(n)$  must be recomputed often, which might lead to unacceptably high computational complexity. We will later discuss the required update rate in relation to the coherence time.

To circumvent this problem, a *long-term* basis  $\mathbf{B}_{\text{KLT}}$  may be defined. For that, we regard  $\mathbf{h}(n, \ell)$  as a Gaussian stationary stochastic vector process with zero-mean. Then

$$\mathbf{R}_a = \mathbb{E}[\mathbf{h}(n, \ell)\mathbf{h}^H(n, \ell)] \quad (8)$$

is the covariance matrix of  $\mathbf{h}(n, \ell)$ , which admits an eigenvalue decomposition (EVD)

$$\mathbf{R}_a = \mathbf{T}\mathbf{\Lambda}\mathbf{T}^H, \quad (9)$$

where  $\mathbf{T} = [\mathbf{t}_1 \cdots \mathbf{t}_M] \in \mathbb{C}^{M \times M}$  is a unitary matrix and  $\mathbf{\Lambda} \in \mathbb{R}^{M \times M}$  is a diagonal matrix  $\lambda_1 \geq \dots \geq \lambda_M \geq 0$ . It can be shown [14] that the representation basis of rank  $p$  that minimizes the mean-squared error (MSE)

$$\text{MSE} = \frac{1}{M} \mathbb{E} [\|(\mathbf{I} - \mathbf{B}\mathbf{B}^H)\mathbf{h}\|_F^2] \quad (10)$$

can be obtained from the Karhunen-Loève transform (KLT) of  $\mathbf{h}(n, \ell)$  as

$$\mathbf{B}_{\text{KLT}} = [\mathbf{t}_1 \cdots \mathbf{t}_p]. \quad (11)$$

The minimum MSE is then

$$\text{MMSE} = \frac{1}{M} \sum_{i=p+1}^r \lambda_i, \quad (12)$$

where  $r \leq M$  is the rank of  $\mathbf{R}_a$ . Obviously, using  $\mathbf{B}_{\text{KLT}}$  results in a larger MSE compared to  $\mathbf{B}_{\text{SVD}}$ . However,  $\mathbf{B}_{\text{KLT}}$  is, in general, a slower (or much slower) changing basis.

### B. Representation Basis in Real Propagation Environments

We assume that channel state information (CSI) corresponding to the most recent  $W$  snapshots is available, and thus approximate  $\mathbf{R}_a(n)$  in (8) by the sample covariance matrix

$$\hat{\mathbf{R}}_a(n) = \frac{1}{W} \sum_{i=0}^{W-1} \frac{1}{L} \mathbf{A}(n-i)\mathbf{A}^H(n-i). \quad (13)$$

The associated representation basis  $\mathbf{B}_a(n)$  is then obtained by extracting the eigenvectors of the  $p$  strongest eigenmodes of  $\hat{\mathbf{R}}_a(n)$ . Note that  $W = 1$  gives  $\mathbf{B}_a(n) = \mathbf{B}_{\text{SVD}}(n)$ , while  $\mathbf{B}_a(n)$  approaches  $\mathbf{B}_{\text{KLT}}(n)$  as  $W$  grows to infinity.

Here a comment is in order. In (13), the model without additive noise (2) has been assumed. This assumption is certainly reasonable for long-term basis, for which we expect  $\mathbf{B}_{\text{KLT}}(n)$  to be stable over many coherence times. Hence, it can be obtained relatively easily from noisy observations (1). For short-term basis, more sophisticated subspace estimation and tracking algorithms may be required. A discussion of such algorithms is, however, beyond the scope of this paper, and we restrict ourselves to merely investigating performance achievable under the assumption that  $\mathbf{B}_{\text{SVD}}(n)$  can be estimated with arbitrarily good accuracy.

We ask the following question: for fixed  $p$  and  $W$ , what can  $\mathbf{B}_a(n)$  tell us about  $\mathbf{h}(n + \Delta n)$ ? Here,  $\Delta n = 0, 1, \dots$  is the *prediction step* size (in our measurements,  $\Delta n = 1$  roughly corresponds to 59 ms). To answer this question, we introduce the normalized captured channel energy

$$\text{NE}(\Delta n) = \frac{1}{N-W-\Delta n+1} \sum_{n=W}^{N-\Delta n} \frac{\|\mathbf{B}_a^H(n)\mathbf{A}(n+\Delta n)\|_F^2}{\|\mathbf{A}(n)\|_F^2}, \quad (14)$$

as a figure of merit.  $\text{NE}(\Delta n)$  can be interpreted as the average fraction of the channel energy that the sequence of bases  $\{\mathbf{B}_a(n)\}_{n=W}^{N-\Delta n}$  can capture  $\Delta n$  snapshots into the future. For the sake of brevity,  $\{\mathbf{B}_a(n)\}_{n=W}^{N-\Delta n}$  will be denoted simply as  $\mathbf{B}_a$  in the sequel.

As a benchmark, it is interesting to examine the performance of the representation bases obtained by considering the correlation of the channel across *subcarriers*. We denote these bases by  $\mathbf{B}_f$ , and compute them from the sample covariance matrix

$$\hat{\mathbf{R}}_f(n) = \frac{1}{W} \sum_{i=0}^{W-1} \frac{1}{M} \mathbf{A}^T(n-i)\mathbf{A}^*(n-i). \quad (15)$$

Such bases have been extensively investigated in, .e.g., [15].

The left-hand side of Fig. 3 shows NE as a function of  $p$  for two cases,  $W = 1$  (a short-term basis) and  $W = 100$  (a long-term basis), and for some selected values of  $\Delta n$ . On the right-hand side of Fig. 3, the corresponding plots for the representation bases  $\mathbf{B}_f$  are also shown. Clearly,  $\mathbf{B}_f$  are more efficient than  $\mathbf{B}_a$ , as they capture more energy for the same  $p$ . Nevertheless,  $\mathbf{B}_a$  can also be regarded as an efficient sequence of bases. For example, Fig. 3 reveals that a long-term basis with  $W = 100$  and  $p = 8$  exists that can capture about 88% of the channel energy. Alternatively, if  $\mathbf{B}_a(n)$  is known for all  $n = 1, \dots$ , the short-term bases with  $W = 1$  and  $p = 8$  can capture 98% of the channel

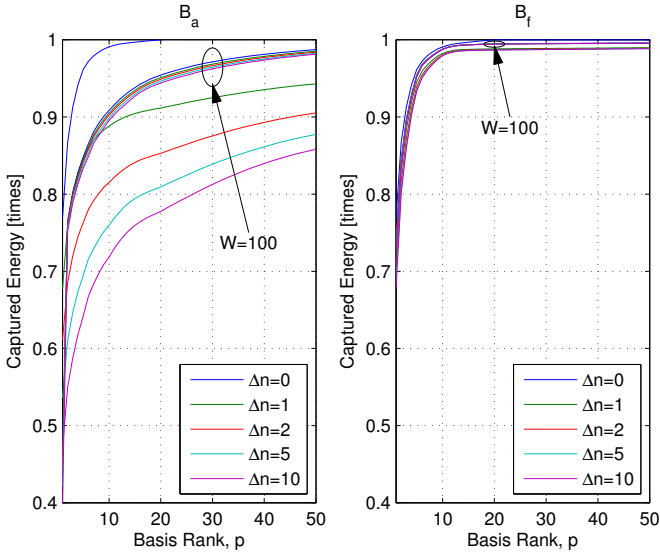


Fig. 3. Normalized captured channel energy  $NE(\Delta n)$  as a function of the basis size  $p$ , for one short-term basis ( $W = 1$ ) and one long-term basis ( $W = 100$ ), and for some selected values of the prediction step size  $\Delta n$ . This example corresponds to the measured outdoor environment.

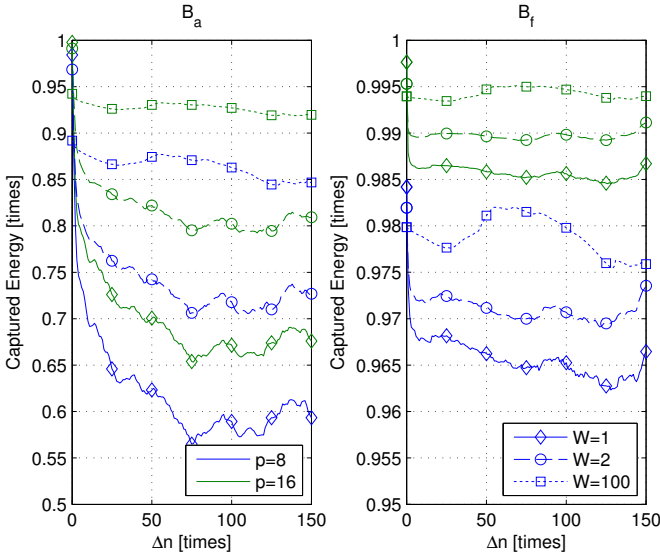


Fig. 4. Normalized captured channel energy  $NE(\Delta n)$  for two short-term bases ( $W = 1$ ,  $W = 2$ ) and one long-term basis  $W = 100$ , and for some selected values of the basis size  $p$ . This example corresponds to the measured outdoor environment. Note that the legends are shared.

energy. The bases  $B_a$  are particularly valuable in situations in which subcarrier correlation cannot be readily exploited. Such situations include, e.g., distributed pilot allocations, or allocations in which pilots are separated beyond the channel coherence bandwidth or time.

Next, we look at the stability of  $B_a$ . Fig. 4 depicts  $NE(\Delta n)$  for two basis sizes,  $p = 8$  and  $p = 16$ , and three observation window lengths,  $W = 1$ ,  $W = 2$  and  $W = 100$ . It is apparent from Fig. 4 that a tradeoff exists between basis efficiency and basis stability. For example, Fig. 4 shows that short-term basis ( $W = 1, 2$ ) achieve efficiency values close to 1, but only

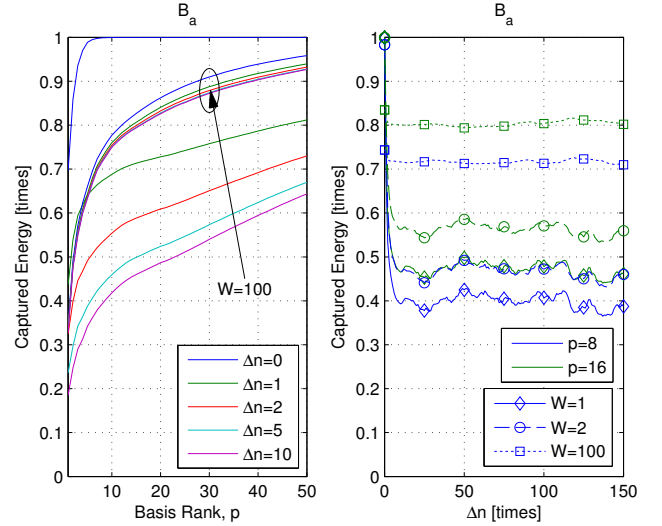


Fig. 5. To the left,  $NE(\Delta n)$  as a function of the basis size  $p$ , for one short-term basis ( $W = 1$ ) and one long-term basis ( $W = 100$ ), and for selected values of the prediction step size  $\Delta n$ . To the right,  $NE(\Delta n)$  for two short-term bases ( $W = 1$ ,  $W = 2$ ) and one long-term basis  $W = 100$ , and for some selected values of the basis size  $p$ . This example corresponds to the measured indoor environment.

when used within one coherence time interval. By contrast, if an observation window of roughly 6 seconds is adopted, the resulting long-term basis can be reused, totally unchanged, for the next 9 seconds, perhaps longer. An explanation to this remarkable observation was suggested in Sec. III where it was argued that, in the measurement setup considered, most of the energy propagates through a limited number of independent paths. In general, short-term bases can accurately capture the local properties of the channel, thus providing efficient bases at the expense of stability. On the other hand, long-term bases can capture well the global properties of the channel, yielding stable but less efficient bases.

Lastly, we briefly compare the performance of the bases  $B_a$  in indoor scenarios (Fig 5) and in outdoor scenarios (Fig 3 and Fig. 4). The main observation is that, in the investigated scenarios,  $B_a$  is less efficient in indoor situations. This can be explained by the larger angular spreads present in indoor environments due to more interactions with walls and furniture.

## V. AN APPLICATION TO CHANNEL ESTIMATION

In this section, we investigate a rank- $p$  vector-scalar LMMSE channel estimator that exploits the antenna correlation of the channel, and evaluate its performance on measured channels. The investigated estimator is pertinent to massive MIMO systems, and it is most attractive in situations in which the frequency correlation of the channel cannot be utilized, e.g., when the distance between pilots is larger than the channel coherence bandwidth or time, or when pilots are allocated in a distributed fashion. In addition, the investigated estimator can also be used to improve the performance of conventional channel estimators, which customarily operate by cascading two one-dimensional filters on the time and frequency dimensions.

### A. Short-Term and Long-Term Channel Estimators

We first introduce some general expressions that apply to LMMSE estimators and reduced-rank LMMSE estimators, which we then tailor to the short-term and long-term cases at hand. We assume that (i) uplink channel estimation is carried out independently for each user; and (ii) pilot transmissions from each user are orthogonal to pilot and data transmissions from other users. We can therefore use the signal model (1) for our channel estimation problem, where  $\mathbf{h}(n, \ell)$  is now a stationary stochastic vector process, and  $s(n, \ell)$  is a known complex scalar. Without loss of generality, we assume that  $s(n, \ell) = 1$ . For the sake of notational simplicity, indices  $n$  and  $\ell$  will be dropped when there is no risk of confusion.

With the signal model (1), the least-squares (LS) estimator of  $\mathbf{h}$  is given by

$$\hat{\mathbf{h}}_{\text{LS}} = \mathbf{y}, \quad (16)$$

while the corresponding LMMSE estimator is

$$\hat{\mathbf{h}}_{\text{LMMSE}} = \mathbf{C}_a(\mathbf{C}_a + N_0\mathbf{I})^{-1}\hat{\mathbf{h}}_{\text{LS}}, \quad (17)$$

where  $\mathbf{C}_a$  will be defined later. At present, we will simply assume that  $\mathbf{C}_a$  admits an EVD  $\mathbf{C}_a = \mathbf{U}\mathbf{\Lambda}\mathbf{U}^H$ , where  $\mathbf{U} = [\mathbf{u}_1 \cdots \mathbf{u}_M] \in \mathbb{C}^{M \times M}$  is a unitary matrix and  $\mathbf{\Lambda} \in \mathbb{R}^{M \times M}$  is a diagonal matrix  $\lambda_1 \geq \dots \geq \lambda_M \geq 0$ . If  $\mathbf{h}$  is a Gaussian process, then estimator (17) is optimal and attains the minimum MSE, given by

$$\text{MMSE} = \frac{1}{M} \sum_{i=1}^r \left( \frac{1}{\lambda_i} + \frac{1}{N_0} \right)^{-1}, \quad (18)$$

where  $r$  is the rank of  $\mathbf{C}_a$ .

The LMMSE estimator (17) has a complexity of  $M^2$  complex multiplications per estimated vector<sup>1</sup>, which in systems with a large number of antennas, might be considered excessive. To address this issue, an optimal rank- $p$  LMMSE estimator is derived in [14], [15] as

$$\hat{\mathbf{h}}_p = \mathbf{U}_p \mathbf{\Sigma}_p \mathbf{U}_p^H \hat{\mathbf{h}}_{\text{LS}}, \quad (19)$$

where  $\mathbf{U}_p = [\mathbf{u}_1 \cdots \mathbf{u}_p] \in \mathbb{C}^{M \times p}$  and  $\mathbf{\Sigma}_p \in \mathbb{R}^{p \times p}$  is a diagonal matrix with entries  $[\frac{\lambda_i}{\lambda_i + N_0}]_{ii}$ ,  $i = 1, \dots, p$ . By using (19), the complexity is reduced to  $2Mp$  complex multiplications per estimated vector. Since (19) only considers the  $p$  strongest eigenmodes of  $\mathbf{C}_a$ , its associated MSE is

$$\text{MSE}(p) = \frac{1}{M} \sum_{i=1}^p \left( \frac{1}{\lambda_i} + \frac{1}{N_0} \right)^{-1} + \frac{1}{M} \sum_{i=p+1}^r \lambda_i. \quad (20)$$

We recognize the second term in the right-hand side of (20) as the representation error (12). This representation error constitutes an error floor that limits the performance of (19) at moderate and high SNR values. To alleviate this situation, we investigate a vector-scalar LMMSE estimator of the form

$$\tilde{\mathbf{h}}_p = \mathbf{U}_p \mathbf{\Sigma}_p \mathbf{U}_p^H \hat{\mathbf{h}}_{\text{LS}} + \alpha(\mathbf{I} - \mathbf{U}_p \mathbf{U}_p^H) \hat{\mathbf{h}}_{\text{LS}}. \quad (21)$$

<sup>1</sup>When computing the complexity of the estimator, the cost of the SVD has been left out. This cost can be charged, instead, to the subspace estimation and tracking algorithms. As argued earlier, we expect that more sophisticated algorithms are needed for the case of short-term bases.

It can be shown that, by selecting the scalar  $\alpha$  as

$$\alpha = \left( \sum_{i=p+1}^r \lambda_i \right) / \left( \sum_{i=p+1}^r \lambda_i + \sum_{i=p+1}^M N_0 \right), \quad (22)$$

the error floor in (20) can be removed, and

$$\begin{aligned} \widetilde{\text{MSE}}(p) &= \frac{1}{M} \sum_{i=1}^p \left( \frac{1}{\lambda_i} + \frac{1}{N_0} \right)^{-1} + \\ &\quad \frac{1}{M} \left( \left( \sum_{i=p+1}^r \lambda_i \right)^{-1} + \left( \sum_{i=p+1}^M N_0 \right)^{-1} \right)^{-1} \end{aligned} \quad (23)$$

is attained. The complexity of this estimator is  $M(2p+1)$  complex multiplications per estimated vector. To see this, simply rewrite (21) as

$$\tilde{\mathbf{h}}_p = \sum_{i=1}^p (\Sigma_{ii} - \alpha) \mathbf{u}_p \mathbf{u}_p^H \hat{\mathbf{h}}_{\text{LS}} + \alpha \hat{\mathbf{h}}_{\text{LS}}.$$

Next, we define  $\mathbf{C}_a$  for the two studied cases of short-term and long-term representation bases.

1) *Short-Term Channel Estimator*: In this case, we let

$$\mathbf{C}_a(n) = \mathbf{B}_{\text{SVD}}(n) \mathbf{\Theta}(\Delta n) \mathbf{B}_{\text{SVD}}^H(n), \quad (24)$$

where  $\mathbf{B}_{\text{SVD}}(n)$  is computed according to (13) with  $W = 1$  and

$$\mathbf{\Theta}(\Delta n) = \text{diag}(\mathbb{E}[\mathbf{u}_1^H(n) \mathbf{h}(n + \Delta n)], \dots, \mathbb{E}[\mathbf{u}_M^H(n) \mathbf{h}(n + \Delta n)]). \quad (25)$$

In (25), we have assumed that  $\mathbb{E}[\mathbf{u}_m^H(n) \mathbf{h}(n + \Delta n)]$ ,  $m = 1, \dots, M$ , is invariant in  $n$ . If this assumption is fulfilled, the entries of  $\mathbf{\Theta}(\Delta n)$  are easily tracked.

2) *Long-Term Basis*: In this case, we simply let

$$\mathbf{C}_a = \hat{\mathbf{R}}_a, \quad (26)$$

where  $\hat{\mathbf{R}}_a$  is computed according to (13) with  $W = 300$ .

### B. Performance Evaluation with Measured Channels

We evaluate the performance of the channel estimators discussed above. The evaluation is based on data sets obtained from channel measurements in both indoor and outdoor environments at 2.6 GHz. Performance is measured in terms of the MSE, which we compute as

$$\text{MSE}(\Delta n) = \frac{1}{N-1} \sum_{n=1}^{N-1} \frac{1}{M} \|\hat{\mathbf{h}}(n + \Delta n) - \mathbf{h}(n + \Delta n)\|_{\text{F}}^2, \quad (27)$$

where, following (2),  $\mathbf{h}(n)$  is a noiseless observation of the channel, and  $\hat{\mathbf{h}}(n + \Delta n)$  is one of (16), (17), (19) or (21). Channel estimators using both short-term and long-term statistics of the antenna covariance matrix of the channel are evaluated. For the short-term channel estimators,  $\mathbf{C}_a(n)$  is obtained as described in Sec. V-A1, for  $n = 1, \dots, N-1$ . Two prediction step sizes,  $\Delta n = 0$  and  $\Delta n = 1$ , are considered. For the long-term channel estimators, a single matrix  $\mathbf{C}_a$  is computed as indicated in Sec. V-A2, and used for all  $n = 1, \dots, N-1$ .



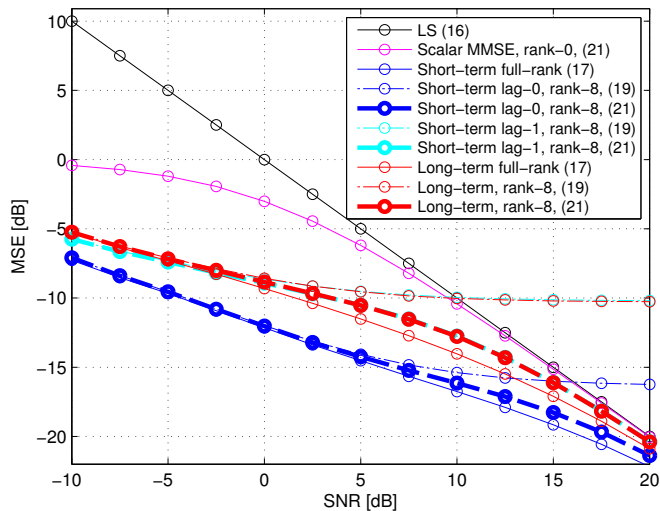


Fig. 6. Performance of antenna correlation based channel estimation in a massive MIMO outdoor setup.

Fig. 6 shows that, when a large number of antennas is available at the BS, antenna correlation based channel estimators can bring about significant gains compared to scalar estimators, specially in the low to medium SNR range. As expected, these gains are larger in the measured outdoor environment compared to the indoor one (not shown due to space constraints). Of particular interest is the rank- $p$  vector-scalar LMMSE channel estimator (21). Careful examination of the plots in Fig. 6 suggests that only a small performance penalty has to be paid by using (21) in place of the optimal LMMSE estimator (17), whereas the computational complexity is reduced by a factor  $M/(2p + 1)$ . Lastly, we compare the performance of channel estimators using short-term and long-term antenna correlation statistics. A key observation is that, in the investigated scenarios, the short-term bases must be updated every coherence time interval in order to outperform the long-term ones. This is difficult since, in reality, channel observations are noisy. Hence, our ability to make use of antenna correlation in massive MIMO for the purpose of channel estimation seems limited to the usage of long-term statistics.

## VI. CONCLUSIONS

In this paper, we investigated the correlation properties of massive MIMO channels with the purpose of obtaining a low-dimensional representation of the channel vectors. We defined short-term and long-term representation bases, and evaluated their performance with data sets obtained from measurements in both indoor and outdoor environments. We found that, within the coherence time of the channel, the short-term bases can capture a larger portion of the channel energy, as compared to the long-term ones. On the other hand, beyond one coherence time and up to several hundred coherence times, the long-term bases offer superior performance. We also investigated a rank- $p$  vector-scalar LMMSE channel estimator that exploits antenna correlation. The investigated estimator has lower complexity, yet performs similarly to the full-rank, optimal LMMSE estimator. Our results also show that, for channel estimation, the short-term bases must be updated every

coherence time interval in order to outperform the long-term ones. This is difficult since, in reality, channel observations are noisy. Hence, our ability to make use of antenna correlation in massive MIMO for the purpose of channel estimation seems limited to the usage of long-term statistics. Future investigations might involve joint-basis for co-located users.

## VII. ACKNOWLEDGMENTS

The authors would like to thank all the participants in this measurement campaign. We would also like to acknowledge the financial support from ELLIIT - an Excellence Center at Linköping-Lund in Information Technology and the Swedish Research Council (VR), as well as the Swedish Foundation for Strategic Research (SSF) and the EU 7<sup>th</sup> Framework Programme under GA n° ICT-619086 (MAMMOET).

## REFERENCES

- [1] T. L. Marzetta, "Noncooperative cellular wireless with unlimited number of base station antennas," *IEEE Trans. Wireless Commun.*, vol. 9, pp. 3590–3600, Nov. 2010.
- [2] F. Rusek, D. Persson, B. K. Lau, E. G. Larsson, T. L. Marzetta, O. Edfors, and F. Tufvesson, "Scaling up MIMO: Opportunities and challenges with very large arrays," *IEEE Signal Process. Mag.*, vol. 30, pp. 40–60, Jan. 2013.
- [3] J. Andrews, S. Buzzi, C. Wan, S. Hanly, A. Lozano, A. Soong, and J. Zhang, "What will 5G be?," *IEEE J. Sel. Areas Commun.*, vol. 32, pp. 1065–1082, June 2014.
- [4] F. Boccardi, R. Heath, A. Lozano, T. Marzetta, and P. Popovski, "Five disruptive technology directions for 5G," *IEEE Commun. Mag.*, vol. 52, pp. 74–80, Feb. 2014.
- [5] N. Junyoung, A. Adhikary, A. Jae-Young, and G. Caire, "Joint spatial division and multiplexing: Opportunistic beamforming, user grouping and simplified downlink scheduling," *IEEE J. Sel. Topics Signal Process.*, vol. 8, pp. 876–890, Mar. 2014.
- [6] A. Adhikary, N. Junyoung, A. Jae-Young, and G. Caire, "Joint spatial division and multiplexing — the large-scale array regime," *IEEE Trans. Inf. Theory*, vol. 59, pp. 6441–6463, June 2013.
- [7] Y. Han, W. Shin, and J. Lee, "Projection based feedback compression for FDD massive MIMO systems," in *Global Telecommunications Conference, GLOBECOM, 2014*, pp. 364–369, Dec. 2014.
- [8] M. S. Sim, J. Park, C. B. Chae, and R. W. Heath, "Compressed channel feedback for correlated massive MIMO systems," *IEEE J. Commun. Netw.*, vol. 18, no. 1, pp. 95–104, 2016.
- [9] J. Joung and S. Sun, "SCF: Sparse channel-state-information feedback using karhunen-loève transform," in *Global Telecommunications Conference, GLOBECOM, 2014*, pp. 314–319, Dec. 2014.
- [10] X. Gao, M. Zhu, F. Rusek, F. Tufvesson, and O. Edfors, "Large antenna array and propagation environment interaction," in *The 48th Annual Asilomar Conference on Signals, Systems, and Computers (ASILOMAR)*, Nov. 2014.
- [11] J. G. Proakis and M. Salehi, *Digital Communications*. Great Britain: McGraw-Hill, 5th Edition, International Edition, 2014.
- [12] J. Flordelis, X. Gao, G. Dahman, F. Rusek, O. Edfors, and F. Tufvesson, "Spatial separation of closely-spaced users in measured massive multi-user MIMO channels," in *Proc. ICC 2015 - IEEE Int. Conf. Commun.*, pp. 1441–1446, June 2015.
- [13] R. S. Thomä, D. Hampicke, A. Richter, G. Sommerkorn, A. Schneider, U. Trautwein, and W. Wornitz, "Identification of time-variant directional mobile radio channels," *IEEE Trans. Instrum. Meas.*, vol. 49, pp. 357–364, Apr. 2000.
- [14] L. L. Scharf and C. C. Demeure, *Statistical signal processing : detection, estimation, and time series analysis*. Addison-Wesley series in electrical and computer engineering, Reading, Mass. Addison-Wesley Pub. Co. cop., 1991.
- [15] O. Edfors, M. Sandell, J.-J. van de Beek, S. K. Wilson, and P. O. Börjesson, "OFDM channel estimation by singular value decomposition," *IEEE Trans. Commun.*, vol. 46, pp. 931–939, July 1998.